Original paper

The study of the interaction of L-cysteine methyl ether with silver salts

E.S. Burlakov[1], D.V. Vishnevetskii[1], E.E. Polyakova[1], D.V. Averkin[2], A.A. Efimov[3], M.Yu. Aleshina[3]

[1]*Tver State University, Tver, Russia*

[2]*Russian Metrological Institute of Technical Physics and Radio Engineering, Solnechnogorsk, Russia*

[3]*Moscow Institute of Physics and Technology, Dolgoprudny, Russia*

rickashet@yandex.ru

DOI: 10.26456/pcascnn/2026.18.811

Abstract: In this work, the effect of silver salts on the self-assembly process in aqueous solutions of L-cysteine methyl ester hydrochloride was studied using UV–visible spectroscopy, dynamic light scattering, electrophoretic light scattering, *pH* measurements, transmission electron microscopy, and selected-area electron diffraction. The nitrate- and acetate-based systems remained visually stable after storage in the dark for 2 months, whereas the nitrite-based systems began to precipitate after several days. The UV-visible spectra showed no characteristic absorption bands and no pronounced scattering region, indicating the stability and homogeneity of the samples. According to the zeta-potential values, the solutions with L-cysteine methyl ester hydrochloride:silver salt ratios of 1:1,5 and 1:1,75 were the most stable in both systems. The dynamic light scattering results showed that only a small number of nanoparticles formed under conditions of silver ion deficiency, whereas an excess of silver ions produced sufficient scattering intensity for reliable particle-size determination. The *pH* measurements revealed different trends for the acetate- and nitrate-based systems. transmission electron microscopy and selected-area electron diffraction data showed that the obtained systems form predominantly amorphous, polydisperse, spherical nanoparticles ranging from 5 to 60 nm in size, with some particles reaching approximately 200 nm.

Keywords: L-cysteine methyl ester, silver nitrate, silver nitrite, silver acetate, self-assembly, nanostructured systems.

Egor S. Burlakov – 1st year postgraduate student, Physical Chemistry Department, Tver State University

Dmitry V. Vishnevetskii – Ph. D., Associate Professor, Physical Chemistry Department, Tver State University, ORCID: 0000-0003-1382-9451

Elizaveta E. Polyakova – graduate student, Leading Engineer, Physical Chemistry Department, Tver State University

Dmitry V. Averkin – Researcher, Laboratory of Metrological Support for Measurements of Dispersed Parameters of Aerosols, Suspensions and Powdery Materials, All-Russian Scientific Research Institute of Physical-Technical and Radiotechnical Measurements, ORCID: 0000-0002-8653-3267

Alexey A. Efimov – Senior Researcher, Head of the Laboratory of Printed and Silicon Microelectronics, Moscow Institute of Physics and Technology, ORCID: 0000-0003-3276-0277

Marina Yu. Aleshina – Junior Researcher, Laboratory of Photonics of Quantum-dimensional Structures, Moscow Institute of Physics and Technology

УДК 544.733.422 *Оригинальная статья*

Изучение взаимодействия L-цистеин метилового эфира с солями серебра

Е.С. Бурлаков[1], Д.В. Вишневецкий[1], Е.Э. Полякова[1], Д.В. Аверкин[2], А.А. Ефимов[3], М.Ю. Алешина[3]

[1]*ФГБОУ ВО «Тверской государственный университет»*
170100, Россия, Тверь, ул. Желябова, 33

[2]*ФГУП «Всероссийский научно-исследовательский институт физико-технических и радиотехнических измерений»,*
141570, Россия, Солнечногорск, пгт. Менделеево, к. 11

© E.S. Burlakov, D.V. Vishnevetskii, E.E. Polyakova, D.V. Averkin, A.A. Efimov, M.Yu. Aleshina, 2026

[3]ФГАОУ ВО «Московский физико-технический институт»
141700, Россия, Московская обл., Долгопрудный, Институтский пер., 9
rickashet@yandex.ru

DOI: 10.26456/pcascnn/2026.18.811

Аннотация: Методами УФ-видимой спектроскопии, динамического рассеяния света, электрофоретического рассеяния света, *pH*-метрии, просвечивающей электронной микроскопии и электронной дифракцией на выбранном участке было исследовано влияние солей серебра на процесс самосборки в водном растворе L-цистеин метилового эфира гидрохлорида. Нитратные и ацетатные системы визуально устойчивы после 2 месяцев при стоянии в покое в отсутствии света, в то время как нитритные начинают выпадать в осадок уже через пару дней. На УФ-спектрах не фиксируются характеристические полосы поглощения, при этом область рассеяния отсутствует, что говорит о стабильности и гомогенности образцов. Согласно значениям дзета-потенциала оказалось, что наиболее стабильными являются растворы с соотношениями L-цистеин метиловый эфир гидрохлорид:соль серебра 1:1,5 и 1:1,75 в обеих системах. Результаты динамического рассеяния света показали, при недостатке ионов серебра образуется малое количество наночастиц, а в избытке ионов серебра их достаточно для определения размеров частиц. Результаты измерения водородного показателя различны для ацетатной и нитратной систем. Данные электронной микроскопии и дифрактографии показывают, что в полученных системах формируются аморфные полидисперсные наночастицы сферической формы размерами от 5 до 60 нм, а некоторые достигают 200 нм.

Ключевые слова: L-цистеин метиловый эфир, нитрат серебра, нитрит серебра, ацетат серебра, самосборка, наноструктурированные системы.

Бурлаков Егор Сергеевич – аспирант 1 года обучения, кафедра физической химии, ФГБОУ ВО «Тверской государственный университет»
Вишневецкий Дмитрий Викторович – к.х.н., доцент кафедры физической химии, ФГБОУ ВО «Тверской государственный университет»
Полякова Елизавета Эдуардовна – магистрант, ведущий инженер кафедры физической химии, ФГБОУ ВО «Тверской государственный университет»
Аверкин Дмитрий Вадимович – научный сотрудник лаборатории метрологического обеспечения измерений дисперсных параметров аэрозолей, взвесей и порошкообразных материалов, ФГУП «Всероссийский научно-исследовательский институт физико-технических и радиотехнических измерений»
Ефимов Алексей Анатольевич – старший научный сотрудник, заведующий лабораторией печатной и кремниевой микроэлектроники, ФГАОУ ВО «Московский физико-технический институт»
Алешина Марина Юрьевна – младший научный сотрудник лаборатории фотоники квантово-размерных структур, ФГАОУ ВО «Московский физико-технический институт»

Поступила в редакцию/received: 12.06.2026; после рецензирования/revised: 29.06.2026; принята/accepted: 01.07.2026.

1. Introduction

Supramolecular gels based on low-molecular-weight gelators (LMWGs) are formed through non-covalent interactions and represent nanostructured systems in which a solid-like supramolecular gel network immobilizes a liquid-like solvent [1]. In such gels, structural information is transferred from the molecular level through self-assembly across multiple length scales, from the nanoscale to the macroscopic level, thereby determining the physical properties of the gel. In recent years, supramolecular gels have been recognized as excellent model systems for studying dynamic self-assembly, opening up opportunities for supramolecular design and for the development of new materials, or materials with improved properties, for various applications [2].

A class of such systems comprises metal-ion-containing gels, or metallogels, which can be formed either by binding metal ions to a preformed gel network or through self-assembly of the initial low-molecular-weight gelator precursors [3]. Some metallogels are coordination-polymer structures, in which metal–ligand coordination enables the formation of extended polymeric chains [4]. McNeil and co-workers demonstrated that LMWGs can be used to reduce metal ions. In their study, $Hg(II)$ cations were used to initiate gelation of a quinoxalinone derivative, with a 1:2 metal-ligand complex forming during the self-assembly process [5]. Although direct ligand binding is one of the simplest approaches to metal immobilization, other strategies are also available. For example, DBS-acylhydrazide has been used to remove precious metal ions, including $Pd(II)$, $Au(III)$, $Ag(I)$, and $Pt(II)$, from aqueous media [6]. These metal ions were spontaneously reduced by the acylhydrazide groups to their zero-valent state, forming nanoparticles entrapped within the gel network [7].

Rizzo and co-workers demonstrated that sugar-based supramolecular gels can remove $Cr(VI)$ ions from wastewater at neutral pH. In these systems, the sugar units play a dual role: they bind chromium-based oxoanions through hydrogen bonding and act as reducing agents, converting toxic $Cr(VI)$ to $Cr(III)$ [8].

Basak and co-workers explored an alternative mechanism for metal immobilization by synthesizing a gel from tripeptide molecules containing repeating phenylalanine units. After self-assembly, this gel was able to undergo contraction, or syneresis. The authors suggested that the hydrophobic phenylalanine units were responsible for gel shrinkage and solvent expulsion. They further demonstrated the applicability of this gel for removing Pb(II) ions from solution [9].

Previously, an unusual self-assembly process involving aqueous solutions of L-cysteine and N-acetyl-L-cysteine with various silver salts was investigated. These systems are capable of forming hydrosols, which undergo a transition to supramolecular thixotropic gels upon the addition of electrolytes such as metal salts [10]. It was found that both the chemical nature of the amino acid and that of the silver salt affect the colloidal and dispersion characteristics of the resulting systems, which in turn influence their biological activity and their ability to acquire additional functional properties [11-13]. A literature survey revealed no reports on self-assembly processes involving an L-cysteine derivative with an esterified carboxyl group, namely L-cysteine methyl ester hydrochloride (L-CMEH), and silver salts. Therefore, the aim of this work was to investigate how the chemical nature of the silver salt affects its interaction with an aqueous solution of L-CMEH.

2. Objects and methods of research

The following reagents were used in this work: *L*-cysteine methyl ester hydrochloride (L-CMEH, 98%, Macklin), silver nitrate (99%, RedOx), silver nitrite (99%, Macklin), and silver acetate (99,95%, Aladdin).

All solutions were prepared using double-distilled water. The samples were prepared as follows. Aqueous solutions of L-CMEH and the corresponding silver salt were first prepared at a concentration of 10 mM. The required volume of water was then added to an empty vial, followed by the addition of the L-CMEH solution and the silver salt solution in ratios, presented in Table 1. The resulting solutions were kept in a dry, dark place until maturation was complete.

Table 1. Sample preparation method.

L-CMEH/silver salt	Water, ml	L-CMEH, ml	Silver salt, ml	C (Ag^+), mM
1:0,25	1,25	0,6	0,15	0,75
1:0,5	1,1	0,6	0,3	1,5
1:0,75	0,95	0,6	0,45	2,25
1:1	0,8	0,6	0,6	3
1:1,25	0,65	0,6	0,75	3,75
1:1,5	0,5	0,6	0,9	4,5
1:1,75	0,35	0,6	1,05	5,25
1:2	0,2	0,6	1,2	6

Electronic absorption spectra were recorded using an SF-2000 spectrophotometer (OKB Spectr). The measurements were performed in glass cuvettes with an optical path length of 5 mm. Particle size measurements in the studied solutions were performed using a Zetasizer Nano ZS analyzer (Malvern). All measurements were carried out at 25°C in the backscattering configuration (173°). The correlation function was processed using Zetasizer Software and the cumulant method. The resulting output was the particle size distribution function, $z(D)$. The hydrodynamic radii of the scattering particles were calculated from the diffusion coefficients using the Stokes–Einstein equation:

$$D = \frac{k \cdot T}{6 \cdot \pi \cdot \eta \cdot R}, \quad (1)$$

where D is the diffusion coefficient; k is the Boltzmann constant; T is the absolute temperature; η is the viscosity of the medium; and R is the radius of the scattering particles.

The zeta potential of the particles in the samples was measured using Malvern DTS1070 U-shaped capillary cuvettes. The relationship between the electrophoretic mobility of the particles and their zeta potential was evaluated using Smoluchowski theory, as implemented in the Zetasizer Nano ZS software and expressed by equation:

$$\zeta = \frac{\mu \cdot \eta}{\varepsilon \cdot \varepsilon_0} \quad (2)$$

where ε is the relative permittivity of the medium; μ is the electrophoretic mobility; ε_0 is the electric constant; η is the dynamic viscosity; and ζ is the zeta potential.

The pH of the solutions was measured using a pH-410 pH meter (Akvilon). TEM images and selected-area electron diffraction (SAED) patterns were obtained using a JEM-2100 transmission electron microscope (JEOL Ltd.) operated at an accelerating voltage of 200 kV.

3. Results and their discussion

Hereafter, only the results obtained for systems with a fixed L-CMEH concentration are discussed, as they were similar to those obtained for systems with a fixed silver ion concentration. First, the long-term stability of the systems was evaluated. The results showed that, in the presence of excess silver ions, the nitrite-based samples changed color within 10 min (see fig. 1 a) and precipitated within several days. After 1 month, the remaining nitrite-based samples also precipitated (see fig. 1 b). Owing to their instability, these systems were not investigated further. By contrast, the nitrate- and acetate-based samples showed no color changes within the first minutes or even after several days and retained good stability after 1 month (see fig. 1 b). However, after 2 months, the acetate-based samples with L-CMEH salt ratios of 1:1,75 and 1:2 also precipitated (see fig. 1 c). All nitrate-based samples remained stable over the same period (see fig. 1 c). The same behavior was observed for systems with a fixed silver ion concentration.

According to the UV-visible spectra (see fig. 2 a, 2 b), no distinct characteristic absorption bands were observed; however, with increasing the silver ion concentration in the system, the spectra shifted toward the long-wavelength region. The absence of a pronounced scattering region indicates the stability and homogeneity of the samples.

The obtained particle distributions by ζ-potential (see fig. 3 a, 3b) showed that systems deficient in silver ions exhibited polymodal distributions and low ζ-potential values. In contrast, under conditions of excess silver ions, the ζ-potential increased and the particle distributions became unimodal. The most stable systems were those with L-CMEH salt ratios of 1:1,5 and 1:1,75, with ζ-potential values reaching 63 mV for the nitrate-based system and 34 and 47 mV, respectively, for the acetate-based system. Systems with a twofold excess of silver ions also exhibited high ζ-potential values; however, their distributions remained polymodal.



Fig. 1. Visual appearance of the systems based on L-CMEH and silver salts (nitrate, nitrite, and acetate, respectively) after 1 day (a), 1 month (b), and 2 months (c) after mixing the precursors.

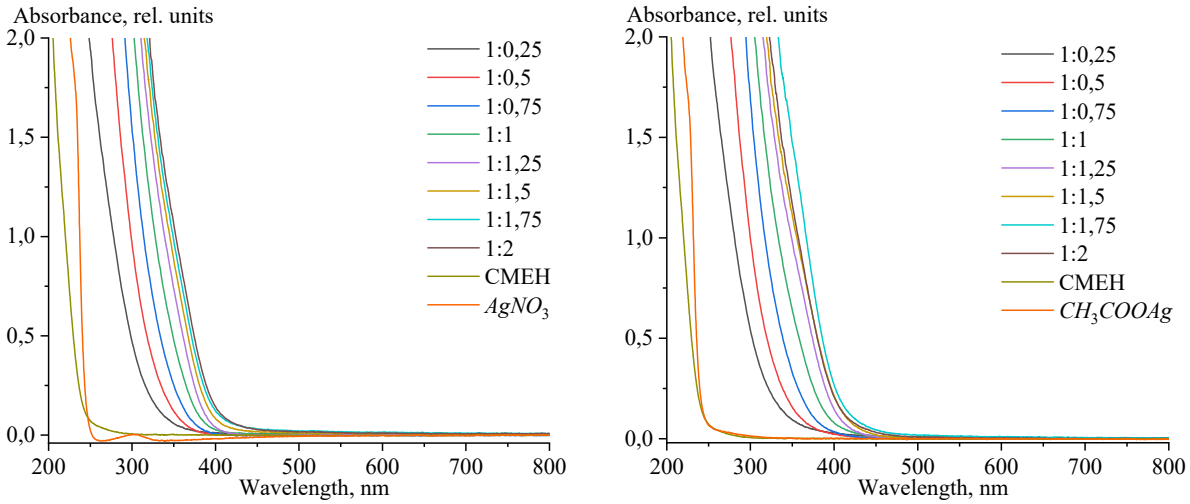

Fig. 2. UV-visible spectra of the L-CMEH/ $AgNO_3$ (a) and L-CMEH/ $AgOOCCH_3$ (b) systems.

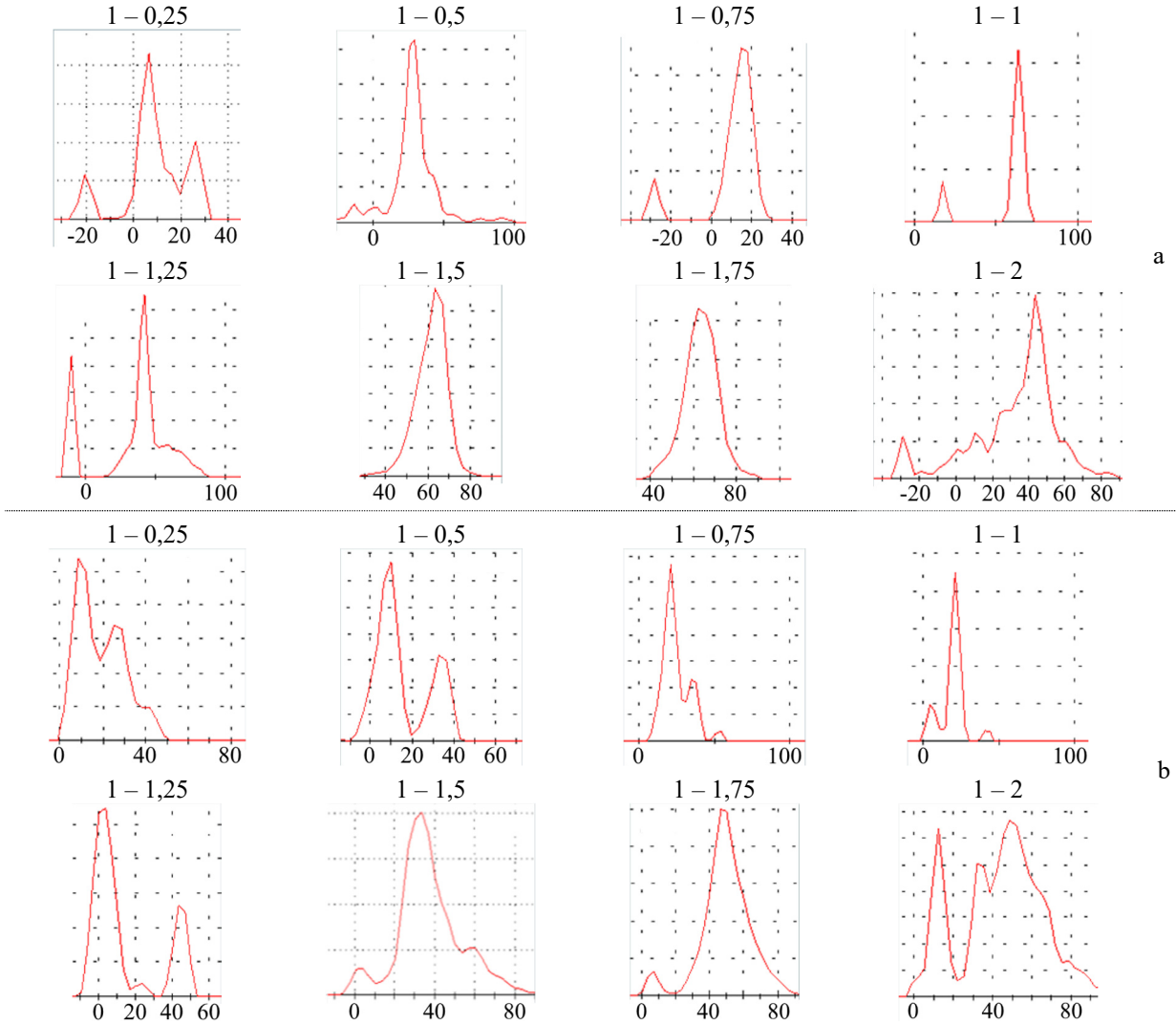

Fig. 3. Particle ζ -potential distributions (mV) for the L-CMEH/ $AgNO_3$ (a) and L-CMEH/ $AgOOCCH_3$ (b) systems.

The dependence of ζ-potential on silver ion concentration shows that the ζ-potential generally increases with increasing silver ion concentration, although the actual trend is rather complex and similar for both systems (see fig. 4 a). At the same time, the electrical conductivity increases in the nitrate-based system but decreases in the acetate-based system (see fig. 4 b), which may be associated with the formation of larger nanoparticles in the acetate-based system compared with the nitrate-based one.

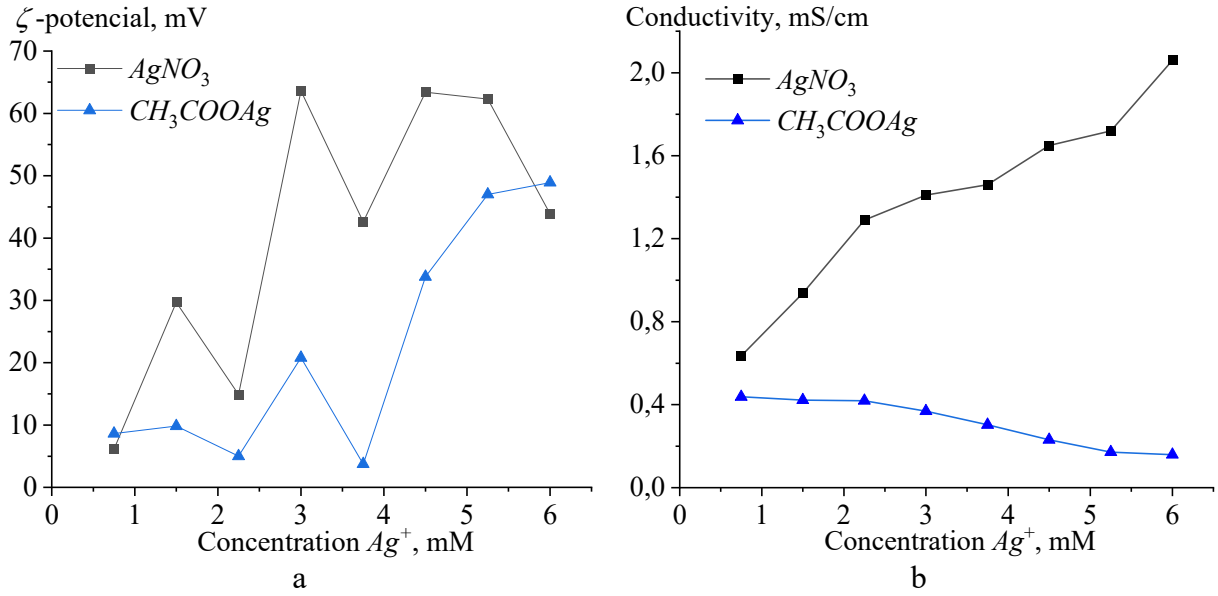

Fig. 4. Dependence of (a) ζ-potential and (b) electrical conductivity on silver ion concentration for the L-CMEH/ $AgNO_3$ and L-CMEH/ $AgOOCCH_3$ systems.

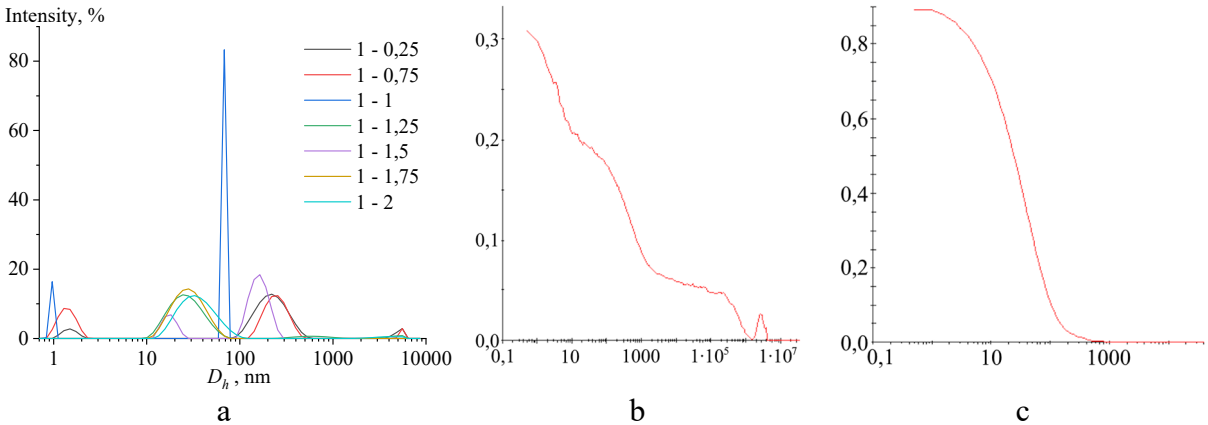

Fig. 5. Particle size distribution for the L-CMEH/ $AgNO_3$ system (a). Cross-correlation function plots for the L-CMEH/ $AgNO_3$ system at precursor ratios of 1:0,75 (b) and 1:1,25 (c), respectively.

As shown in fig. 5 a, the particle size distribution is bimodal under conditions of silver ion deficiency. However, analysis of the cross-correlation function (see fig. 5 b) indicates that the nanoparticle concentration in the system

is extremely low; therefore, applying the cumulant method to this function provides only a rough estimate of the size of the particles formed. In the presence of excess silver ions, the cross-correlation function becomes smoother (see fig. 5 c), the light scattering amplitude increases markedly, and cumulant analysis reveals a unimodal particle size distribution.

For the acetate-based system (see fig. 6 a), the results were similar; however, well-defined cross-correlation functions were obtained only for samples with initial reagent ratios of 1:1,75 and 1:2 (see fig. 6 b, c). The DLS results correlated well with the ELS data: the nanoparticle size was approximately 25 nm for the nitrate-based system at a precursor ratio of 1:1.75 and approximately 50 nm for the acetate-based system at the same ratio. At the same time, the ζ-potential was higher for the nitrate-based system, which can be explained by the higher surface charge density of the smaller particles.

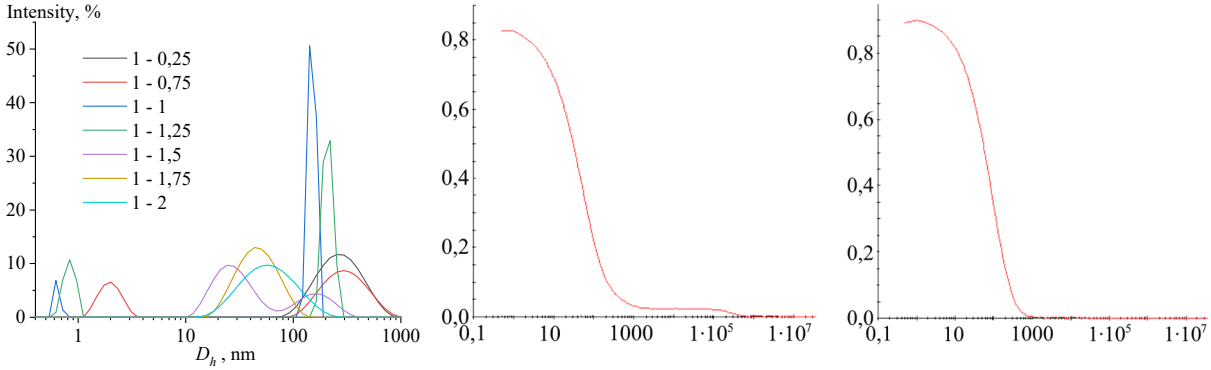

Fig. 6. Particle size distribution for the L-CMEH/ $AgOOCCH_3$ system (a). Cross-correlation function plots for the L-CMEH/ $AgOOCCH_3$ system at precursor ratios of 1:1,5 (b) and 1:1,75 (c), respectively.

As shown in fig. 7, an increase in silver salt concentration leads to a decrease in pH, indicating an increase in solution acidity. This indirectly suggests the substitution of hydrogen ions in the thiol ($-SH$) groups by silver ions. However, the acetate-based system differs from the nitrate-based system: at silver ion concentrations above 3 mM, the pH increases (see fig. 7 b). In this case, the acidity of the solution is governed by the formation of nitric or acetic acid, the former being a strong acid and the latter a weak one.

Preliminary TEM data were obtained only for samples with a precursor ratio of 1:0,75 (see fig. 8, top). The silver nitrate control sample was characterized by pronounced polydispersity and near-spherical particles with no clearly defined facets. The nanoparticle sizes ranged from 5 to 40 nm, while large aggregates reaching approximately 1 μm were also observed. The particles were unevenly distributed over the grid surface, with regions containing a high concentration of nanoparticles as well as areas with single, relatively isolated particles.

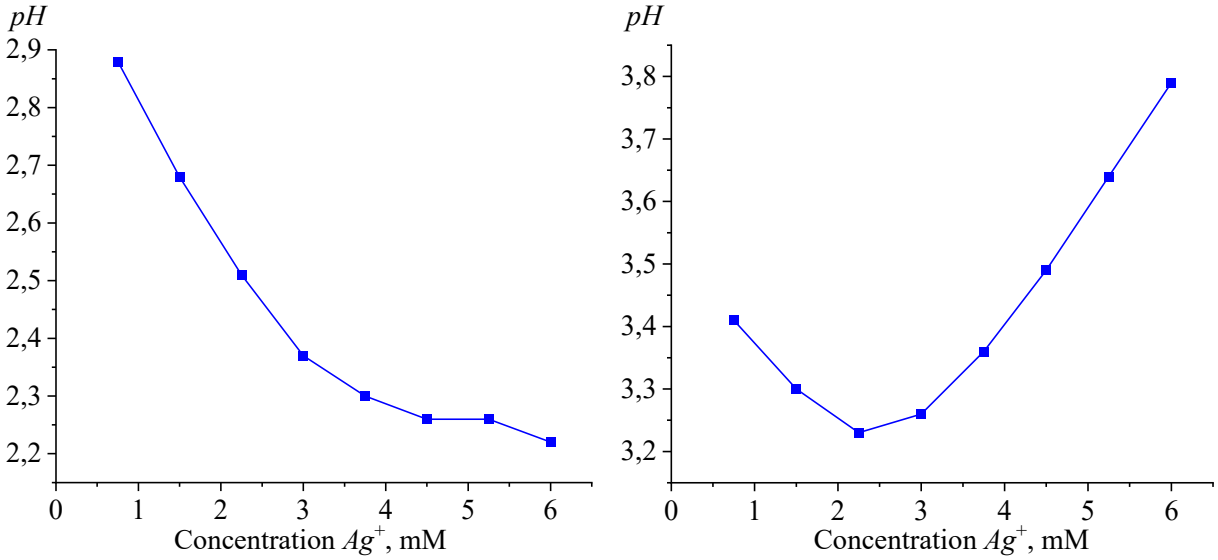

Fig. 7. Dependence of pH on silver ion concentration for the L-CMEH/ $AgNO_3$ (a) and L-CMEH/ $AgOOCCH_3$ (b) systems.

Nanoparticles in the L-CMEH/ $AgNO_3$ system were spherical and showed no pronounced faceting. Their sizes ranged from 6 to 60 nm, with some particles reaching approximately 200 nm. The nanoparticles were unevenly distributed over the grid surface, mainly along the solvent drying boundaries.

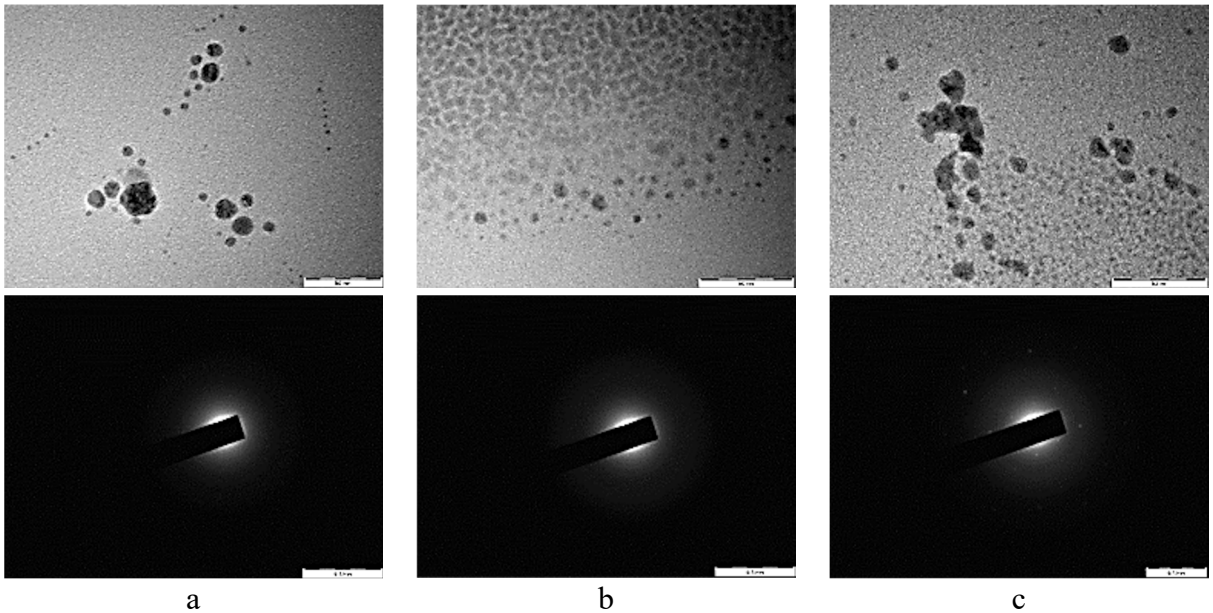

Fig. 8. TEM images (top) and SAED patterns (bottom) of $AgNO_3$ (a), L-CMEH/ $AgNO_3$ (b), and L-CMEH/ $AgOOCCH_3$ (c). Scale bars: 50 nm for the TEM images and 5 nm^{-1} for the SAED patterns.

Particles in the L-CMEH/ $AgOOCCH_3$ system were characterized by pronounced polydispersity and a tendency to aggregate. Most particles were spherical and had no pronounced facets, with individual particles approximately

5-15 nm in size. Their distribution on the carbon substrate was uneven: both isolated nanoparticles and irregularly shaped agglomerates with characteristic sizes ranging from tens to hundreds of nanometers, up to approximately 200 nm, were observed.

According to the SAED analysis (see fig. 8, bottom), the silver nitrate control sample and the nitrate-based system were predominantly amorphous, whereas the acetate-based system exhibited reflections indicating the presence of crystalline inclusions, presumably silver nanoparticles.

5. Conclusions

Our study presents preliminary results on the self-assembly process in mixed aqueous solutions of L-CMEH and different silver salts. The most stable and homogeneous systems were obtained when the silver ion concentration exceeded the L-CMEH concentration. This conclusion is supported by ζ-potential values of 62,3 and 47 mV for the nitrate- and acetate-based systems, respectively, at an L-CMEH:silver salt ratio of 1:1,75. The particle size of the resulting systems was found to differ by approximately 10-20 nm depending on the chemical nature of the silver salt. This trend is supported by DLS data and is consistent with our TEM observations; however, a definitive conclusion cannot yet be drawn because TEM images of the samples with a precursor ratio of 1:1,75 are not available. At the same time, the SAED patterns indicate the formation of some crystalline silver nanoparticles in the acetate-based system, whereas such crystalline phase was not detected in the nitrate-based system.

This research was carried out using the equipment of the Shared Facilities Center at Tver State University.

References:

1. Smith D.K. Supramolecular gels – a panorama of low-molecular-weight gelators from ancient origins to next-generation technologies, *Soft Matter*, 2024, vol. 20, issue 1, pp. 10-70. DOI: 10.1039/D3SM01301D.
2. Sangeetha N.M., Maitra U. Supramolecular gels: functions and uses, *Chemical Society Reviews*, 2005, vol. 34, issue 10, pp. 821-836. DOI:10.1039/B417081B.
3. Tam A.Y.-Y., Tam V.W.-W. Recent advances in metallogels, *Chemical Society Reviews*, 2013, vol. 42, issue 4, pp. 1540-1567. DOI:10.1039/C2CS35354G.
4. Sutar P., Maji T.K. Recent advances in coordination-driven polymeric gel materials: design and applications, *Dalton Transactions*, 2020, vol. 49, issue 23, pp. 7658-7672. DOI: 10.1039/D0DT00863J.
5. King K.N., McNeil A.J. Streamlined approach to a new gelator: inspiration from solid-state interactions for a mercury-induced gelation, *Chemical Communications*, 2010, vol. 46, issue 20, pp. 3511-3513. DOI: 10.1039/C002081H.
6. Okesola B.O., Suravaram S.K., Parkin A., Smith D.K. Selective extraction and in situ reduction of precious metal salts from model waste to generate hybrid gels with embedded electrocatalytic nanoparticles, *Angewandte Chemie, International Edition*, 2016, vol. 55, issue 1, pp. 183-187. DOI: 10.1002/anie.201507684.
7. Albino M., Burden T. J., Piras C. C. et. al. Mechanically robust hybrid gel beads loaded with «naked» palladium nanoparticles as efficient, reusable, and sustainable catalysts for the Suzuki–Miyaura reaction, *ACS Sustainable Chemistry and Engineering*, 2023, vol. 11, issue 5, pp. 1678-1689. DOI: 10.1021/acssuschemeng.2c05484.
8. Rizzo C., Andrews J.L., Steed J.W., D'Anna F. Carbohydrate-supramolecular gels: adsorbents for chromium(VI) removal from wastewater, *Journal of Colloid and Interface Science*, 2019, vol. 548, pp. 184-196.

DOI: 10.1016/j.jcis.2019.04.034.
9. Basak S., Nandi N., Paul S. et. al. A tripeptide-based self-shrinking hydrogel for waste-water treatment: removal of toxic organic dyes and lead (Pb*2*+) ions, *Chemical Communications*, 2017, vol. 53, issue 43, pp. 5910-5913. DOI: 10.1039/C7CC01774J.
10. Vishnevetskii D.V., Averkin D.V., Efimov A.A. et. al. L-cysteine and N-acetyl-L-cysteine mediated synthesis of nanosilver-based sols and hydrogels with antibacterial and antibiofilm properties, *Journal of Materials Chemistry B*, 2023, vol. 11, issue 25, pp. 5794-5804. DOI: 10.1039/D3TB00261F.
11. Vishnevetskii D.V., Polyakova E.E., Andrianova Y.V. et. al. L-cysteine/silver nitrate/iodate anions system: peculiarities of supramolecular gel formation with and without visible-light exposure, *Gels*, 2024, vol. 10, issue 12, pp. 809-824. DOI: 10.3390/gels10120809.
12. Vishnevetskii D.V., Metlin F.A., Polyakova E.E. et. al. Preparation of composite hydrogels based on cysteine–silver sol and methylene blue as promising systems for anticancer photodynamic therapy, *Gels*, 2024, vol. 10, issue 9, pp. 577-593. DOI: 10.3390/gels10090577.
13. Vishnevetskii D.V., Mekhtiev A.R., Averkin D.V., Polyakova E.E. Cysteine–silver–polymer systems for the preparation of hydrogels and films with potential applications in regenerative medicine, *Gels*, 2023, vol. 9, issue 12, pp. 924-936. DOI: 10.3390/gels9120924.

Библиографический список:

1. **Smith, D.K.** Supramolecular gels – a panorama of low-molecular-weight gelators from ancient origins to next-generation technologies / D.K. Smith // Soft Matter. – 2024. – V. 20. – I. 1. – P. 10-70. DOI: 10.1039/D3SM01301D.
2. **Sangeetha, N.M.** Supramolecular gels: functions and uses / N.M. Sangeetha, U. Maitra // Chemical Society Reviews. – 2005. – V. 34. – I. 10. – P. 821-836. DOI: 10.1039/B417081B.
3. Tam A. Y.-Y. Recent advances in metallogels / A. Y.-Y. Tam and V. W.-W. Tam // Chemical Society Reviews. – 2013. – V. 42. – I. 4. – P. 1540-1567. DOI:10.1039/C2CS35354G.
4. **Sutar, P.** Recent advances in coordination-driven polymeric gel materials: design and applications / P. Sutar, T.K. Maji // Dalton Transactions. – 2020. – V. 49 – I. 23. – P. 7658-7672. DOI: 10.1039/D0DT00863J.
5. **King, K.N.** Streamlined approach to a new gelator: inspiration from solid-state interactions for a mercury-induced gelation / K.N. King, A.J. McNeil // Chemical Communications. – 2010. – V. 46. – I. 20. – P. 3511-3513. DOI: 10.1039/C002081H.
6. **Okesola, B.** O. Selective extraction and in situ reduction of precious metal salts from model waste to generate hybrid gels with embedded electrocatalytic nanoparticles / B.O. Okesola, S.K. Suravaram, A. Parkin, D.K. Smith // Angewandte Chemie, International Edition. – 2016. – V. 55. – I. 1. – P. 183-187. DOI: 10.1002/anie.201507684.
7. **Albino, M.** Mechanically robust hybrid gel beads loaded with «naked» palladium nanoparticles as efficient, reusable, and sustainable catalysts for the Suzuki–Miyaura reaction / M. Albino, T.J. Burden, C.C. Piras et. al. // ACS Sustainable Chemistry and Engineering. – 2023. – V. 11. – I. 5. – P. 1678-1689. DOI: 10.1021/acssuschemeng.2c05484.
8. **Rizzo, C.** Carbohydrate-supramolecular gels: adsorbents for chromium(VI) removal from wastewater / C. Rizzo, J.L. Andrews, J.W. Steed, F.D'Anna // Journal of Colloid and Interface Science. –2019. – V. 548. – P. 184-196. DOI:10.1016/j.jcis.2019.04.034.
9. **Basak, S.** A tripeptide-based self-shrinking hydrogel for waste-water treatment: removal of toxic organic dyes and lead (Pb^{2+}) ions / S. Basak, N. Nandi, S. Paul et. al. // Chemical Communications. – 2017. – V. 53. – I. 43. – P. 5910-5913. DOI:10.1039/C7CC01774J.
10. **Vishnevetskii, D.V.** L-cysteine and N-acetyl-L-cysteine mediated synthesis of nanosilver-based sols and hydrogels with antibacterial and antibiofilm properties / D.V. Vishnevetskii, D.V. Averkin, A.A. Efimov et. al. // Journal of Materials Chemistry B. – 2023. – V. 11. – I. 25. – P. 5794-5804. DOI:10.1039/D3TB00261F
11. **Vishnevetskii, D.V.** L-cysteine/silver nitrate/iodate anions system: peculiarities of supramolecular gel formation with and without visible-light exposure / D.V. Vishnevetskii, E.E. Polyakova, Y.V. Andrianova et. al. // Gels. – 2024. – V. 10. – I. 12. – P. 809-824. DOI: 10.3390/gels10120809
12. **Vishnevetskii, D.V.** Preparation of composite hydrogels based on cysteine–silver sol and methylene blue as promising systems for anticancer photodynamic therapy / D.V. Vishnevetskii, F.A. Metlin, E.E. Polyakova et. al. // Gels. – 2024. – V. 10. – I. 9. – P. 577-593. DOI: 10.3390/gels10090577.
13. **Vishnevetskii, D.V.** Cysteine–silver–polymer systems for the preparation of hydrogels and films with potential applications in regenerative medicine / D.V. Vishnevetskii, A.R. Mekhtiev, D.V. Averkin, E.E. Polyakova // Gels. – 2023. – V. 9. – I. 12. – P. 924-936. DOI: 10.3390/gels9120924.